fied by introducing[1] the concept of "admittance matrix" looking into a given region. This procedure does not necessarily facilitate the actual computational work, but establishes a welcome link with network theory. To this effect we introduce a complete set of real orthonormal vectors $\bar{\alpha}_m$ on S', and perform the expansions

$$\bar{E}_t = \sum V_m \bar{\alpha}_m$$

$$\bar{H}_t \times \bar{u}_n = \sum I_m \bar{\alpha}_m.$$

Between the V's and the I's exists the circuit relationship

$$\bar{I} = \mathcal{Y}_0 \cdot \bar{V} \tag{8}$$

where $\mathcal{Y}_0$ is the radiating admittance looking outside S_1. The scalar product takes the form

$$\begin{aligned}\langle \bar{\epsilon}_a, \bar{\epsilon}_b \rangle &= \frac{1}{4}(\bar{V}_a^* \cdot \bar{I}_b + \bar{V}_b \cdot \bar{I}_a^*) \\ &= \frac{1}{4}(\bar{V}_a^* \cdot \mathcal{Y}_0 \cdot \bar{V}_b + \bar{V}_b \cdot \mathcal{Y}_0^* \cdot \bar{V}_a^*) \\ &= \frac{1}{4}\bar{V}_a^* \cdot (\mathcal{Y}_0 + \mathcal{Y}_0^\dagger) \cdot \bar{V}_b \\ &= \frac{1}{2}\bar{V}_a^* \cdot \mathcal{H}_0 \cdot \bar{V}_b \end{aligned} \tag{9}$$

where $\mathcal{H}_0$ is the Hermitian part of $\mathcal{Y}_0$. When the medium outside S_1 is symmetric (i.e., $\epsilon = \tilde{\epsilon}$, $\mu = \tilde{\mu}$, the conductivity being incorporated in ϵ), $\mathcal{Y}_0$ turns out to be symmetric,[2] and its Hermitian part is the conductance matrix $\mathcal{G}_0$. In the absence of energy sources, $\langle \bar{\epsilon}_a, \bar{\epsilon}_a \rangle$ is always positive, hence, $\mathcal{H}_0$ is positive definite. To determine $\bar{V}$, two circuit equations of the type (8) must be written.[1] One obtains, by elimination of $\bar{I}$,

$$\bar{I}_g = (\mathcal{Y}_0 + \mathcal{Y}_i) \cdot \bar{V} \tag{10}$$

where $\mathcal{Y}_i$ is the admittance looking inside S_1. The column vector $\bar{I}_g$ represents the expansion coefficients I_{gm} of the surface current produced by the sources $\bar{J}$ on the short-circuited surface S'. In other words, the current density $\bar{J}_s$ is equal to $\Sigma I_{gm} \bar{\alpha}_m$. Inversion of the $(\mathcal{Y}_0 + \mathcal{Y}_i)$ matrix gives

$$\bar{V} = (\mathcal{Y}_0 + \mathcal{Y}_i)^{-1} \cdot \bar{I}_g = \mathcal{Z}\bar{I}_g. \tag{11}$$

To obtain optimum launching efficiency, this value of $\bar{V}$ should be proportional to the vector $\bar{V}_1$ corresponding to the desired tangential field $\bar{E}_{t1}$. Alternatively, the sources should induce an (optimum) wall-current density

$$\bar{I}_{g1} = (\mathcal{Y}_0 + \mathcal{Y}_i) \cdot \bar{V}_1 \tag{12}$$

We can now express λ in the following form

$$\begin{aligned}\lambda &= \frac{\langle \bar{\epsilon}_1, \bar{\epsilon} \rangle}{\langle \bar{\epsilon}_1, \bar{\epsilon}_1 \rangle} = \frac{\bar{V}_1^* \cdot \mathcal{H}_0 \cdot \bar{V}}{\bar{V}_1^* \cdot \mathcal{H}_0 \cdot \bar{V}_1} \\ &= \frac{(\mathcal{Z}^* \cdot \bar{I}_{g1}^*) \cdot \mathcal{H}_0 \cdot (\mathcal{Z} \cdot \bar{I}_g)}{(\mathcal{Z}^* \cdot \bar{I}_{g1}^*) \mathcal{H}_0 \cdot (\mathcal{Z} \cdot \bar{I}_{g1})} \\ &= \frac{\bar{I}_{g1}^* \cdot [\mathcal{Z}^\dagger \cdot \mathcal{H}_0 \cdot \mathcal{Z}] \cdot \bar{I}_g}{\bar{I}_{g1}^* \cdot [\mathcal{Z}^\dagger \cdot \mathcal{H}_0 \cdot \mathcal{Z}] \cdot \bar{I}_{g1}}. \end{aligned} \tag{13}$$

[1] J. Van Bladel, "The matrix formulation of scattering problems," *IEEE Trans. on Microwave Theory and Techniques*, vol. MTT-14, pp. 130–135, March 1966.

[2] J. Van Bladel, "A generalized reciprocity theorem for radiating apertures," *Arch. Elekt. Übertragung*, pp. 447–450, August 1966.

Equation (13) shows, in principle at least, how to determine the coupling coefficient λ, given the actual short-circuit current $\bar{I}_g$ and its optimum value $\bar{I}_{g1}$. This relationship can also be put in the form of a splitting

$$I_g = \lambda \bar{I}_{g1} + \bar{I}_{g2} \tag{14}$$

where the two parts, $\lambda \bar{I}_{g1}$ and $\bar{I}_{g2}$, are orthogonal with respect to a scalar product

$$\langle \bar{I}_{ga}, \bar{I}_{gb} \rangle = \bar{I}_{ga}^* \cdot [\mathcal{Z}^\dagger \cdot \mathcal{H}_0 \cdot \mathcal{Z}] \cdot \bar{I}_{gb} \tag{15}$$

It is to be noticed that the bracketed matrix is Hermitian.

J. Van Bladel
Laboratory for Electromagnetism
and Acoustics
University of Ghent
Ghent, Belgium

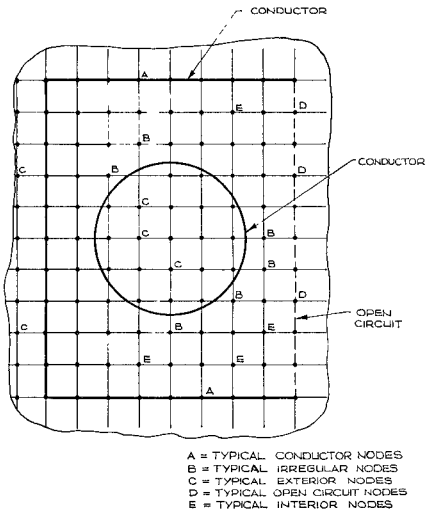

Fig. 1. Finite difference net.

The Numerical Solution of TEM Mode Transmission Lines with Curved Boundaries

Introduction

A finite difference solution of Laplace's equation has been used by several authors [1], [2] to obtain the transmission-line parameters of uniform TEM transmission lines with straight-line boundaries. This correspondence shows that useful results can also be obtained where the finite difference solution is modified to permit curved boundaries.

Theory

Figure 1 shows a finite difference net used to obtain the odd mode transmission line parameters of the transmission line with the cross section shown in Fig. 2. It is seen that four different types of nodes are produced by the net. They are:

a) Conducting nodes such as A
b) Irregular nodes such as B
c) Exterior nodes such as C
d) Open-circuit nodes such as D
e) Interior nodes such as E.

Only the irregular nodes are different from those treated previously [1]. A suitable finite difference approximation for use at irregular nodes is given by Forsythe and Wasaw [3] and Weber [7]:

$$\left(\frac{1}{h_1 h_2} + \frac{1}{h_3 h_4}\right) V_0 = \frac{V_1}{h_1(h_1+h_3)} + \frac{V_2}{h_2(h_2+h_4)} + \frac{V_3}{h_3(h_1+h_3)} + \frac{V_4}{h_4(h_2+h_4)}$$

where the notation is given in Fig. 3.

Although the error in this approximation is of the order $0(h)$ as compared with $0(h^2)$ for interior nodes it has been shown [4] that the overall accuracy is still of the order $0(h^2)$.

Manuscript received August 29, 1966; revised November 15, 1966.

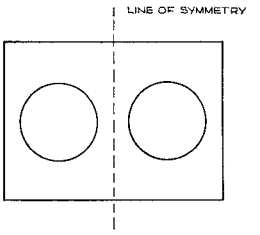

Fig. 2. Transmission line cross section.

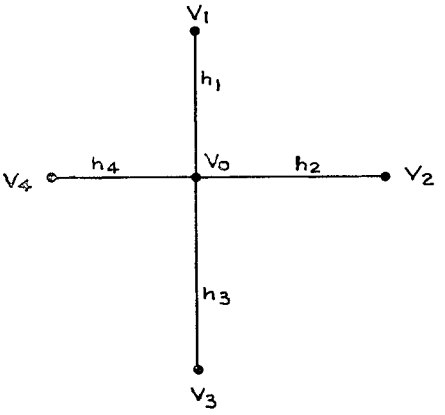

Fig. 3. Notation for irregular nodes.

Programming

To analyze a particular problem the program should only require the boundaries to be specified. This was achieved by scanning all the nodes of the net and suitably tagging each irregular node. All conductor and exterior nodes were also tagged by putting them at an integral value of potential. Successive over-relaxation [1] was used to obtain the approximate potential at each node of the net. The transmission-line parameters were obtained from either Gauss's theorem [1] or the energy [6] which was obtained by interpolating an approximate but continuous potential function satisfying the boundary values.

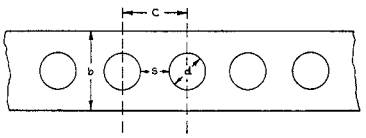

Fig. 4. Coupled rods.

TABLE I

CHARACTERISTIC IMPEDANCE OF COAXIAL LINE AND COUPLED RODS

Coupled Rods

d/b	s/b	Number of Nodes Used	Z_0 from Gauss's Theorem		Lower Bound on Z_0 from Energy Formula		Z_0 from* Cristal [5]	
			Z_0 Even	Z_0 Odd	Z_0 Even	Z_0 Odd	Z_0 Even	Z_0 Odd
0.8	1.5	2170	25.43	25.22	25.44	25.24		25.2
0.6	1.7	2170	44.57	—	44.56	—		
0.6	1.5	1984	44.76	44.13	44.69	44.13	44.7	44.13
0.6	1.5	5460	44.70	44.13	44.70	44.13		
0.6	1.4	1891	—	44.02	—	44.02		
0.4	1.5	1798	69.89	68.69	69.87	68.67	69.87	68.69
0.2	1.5	1612	112.09	109 85	112.04	109.73	112.09	109.82
0.1	0.9	961	163.43	142.62	162.8	142.05		142.6
0.1	0.9	3721	163.40	142.58	163.27	142.5		142.6
0.5	0 5	961	65.52	46.08	65.08	46.09		46.1

Coaxial Line

Diameter Ratio	Number of Nodes Used	Z_0 from Gauss's Theorem	Lower Bound on Z_0 from Energy Formula	Exact Z_0
1.5174	3721	25.0073	25.0019	25.0026
2.0	441	41.5627	41.5333	41.5601
2.0	3721	41.5843	41.5577	41.5601
2.3022	3721	50.0291	49.9947	49.9973
3.4933	3721	75.0351	74.9918	74.9989

* In a private communication Dr. Cristal stated that, in his Table III first case, the three values given by him are Z_0 odd impedances. The Z_0 even impedances he obtained are given in this Table.

RESULTS

The program was used to obtain the characteristic impedance Z_0 of coaxial line and the even and odd mode characteristic impedance (Z_0 even and Z_0 odd) of the coupled rods shown in Fig. 4. The results are given in Table I along with the results obtained for coupled rods by Cristal who numerically solved an integral equation. It is seen that the error in the results is probably much less than 1 percent, and that the error in Cristal's results is probably much less than the 1 percent to 2 percent claimed by him.

CONCLUSION

It has been shown that a finite difference solution of Laplace's equation can give accurate values of the transmission line parameters of uniform TEM transmission lines with curved boundaries.

ACKNOWLEDGMENT

The permission of the Chief Scientist of the Department of Supply to publish this article is acknowledged.

C. T. CARSON
Weapons Research Estab.
Adelaide, Australia

REFERENCES

[1] H. E. Green, "Numerical solution of some important transmission-line problems," *IEEE Trans. on Microwave Theory and Techniques*, vol. MTT-13, pp. 676-692, September 1965.
[2] M. V. Schneider, "Computation of impedance and attenuation of TEM-lines by finite difference methods," *IEEE Trans. on Microwave Theory and Techniques*, vol. MTT-13, pp. 793-800, November 1965.
[3] Forsythe and Wasaw, *Finite Difference Methods for Partial Differential Equations*. New York: Wiley, 1960.
[4] J. H. Bramble and B. E. Hubbard, "New monotype approximations for elliptic problems," *Math. Comput.*, vol. 18, no. 87, July 1964.
[5] E. G. Cristal, "Coupled circular cylindrical rods between parallel ground planes," *IEEE Trans. on Microwave Theory and Techniques*, vol. MTT-12, pp. 428-439, July 1964.
[6] G. K. Campbell and C. T. Carson, "Upper and lower bounds on the characteristic impedance of TEM mode transmission lines," Weapons Research Establishment, Tech. Memo Pad 217.
[7] E. Weber, *Electromagnetic Fields*, vol. 1. New York: Wiley, 1950, p. 263.

A Wideband Coaxial-Line Power Divider

In a recent paper, Parad and Moynihan[1] discussed a strip-line three-port power divider impedance matched in all three ports. Previously, a coaxial-line version of the above type of power divider was developed by Kaplan.[2] This correspondence discusses a method of significantly increasing the bandwidth of this type of device; it is accomplished by open-circuited quarter-wave transmission lines introduced at a novel location within the device. A wideband power divider has been designed, fabricated, and tested; its measured performance over an octave frequency band is presented.

Figure 1 shows the basic configuration of the wideband power divider. Figure 2 shows an internal view of the power divider. It is noted that the square outer conductors of the coaxial lines near all three ports are stepped to circular cross sections to permit use of commercial connectors.

The operation of this type of three-port power divider is easily understood since it is in concept a lossless four-port hybrid junction with a terminated inaccessible difference port. Port 1, the input port, is the sum port; a signal fed in at this port divides into two equal, in-phase outputs at ports 2 and 3, the collinear ports. The inaccessible difference port is located at the end of the dual-mode transmission line (balanced mode) at the junction (on the center line) of the output coaxial lines. If, instead, a signal were to be applied at an output port, it would divide evenly between the unbalanced and balanced modes of the dual-mode line; the opposite output port would be perfectly isolated (no signal would be delivered to it). The signal in the unbalanced mode would be delivered to the sum port; the signal in the balanced mode would be delivered to the difference port and would, of course, be dissipated in the termination.

The design of this hybrid-type power divider is readily optimized by maintaining symmetry and simultaneously matching the sum and difference ports. Since symmetry can always be maintained by precision manufacture, the limitation on bandwidth is caused by the degradations with frequency of the specific matching schemes for the sum and difference ports. For this power divider, or either of the previous ones,[1,2] the reflection at the sum port versus frequency is that of a single stage quarter-wavelength impedance matching transformer; this matches the $\frac{1}{2}$ to 1 resistive discontinuity caused by the output lines which are in parallel across the input line. In the previous designs, the internal termination was directly connected to the difference port; for these cases, the difference port reflection versus frequency is that of the short-circuited quarter-wavelength stub of balanced-mode transmission line in parallel with the termination. This reflection degrades much more rapidly with frequency than that of the sum port; therefore, it is the limitation on bandwidth of these designs.

The essence of this correspondence is the technique for significantly increasing the bandwidth of this type of power divider; it is accomplished by reactive compensation of the reflection of the difference port. The compensation is obtained by introducing open-circuited quarter-wavelength lines in series with the termination; these lines are located inside of the inner conductors of the output coaxial lines, as shown in Fig. 1. The variation of reactance of these series, open-circuited lines tends to cancel that of the parallel, balanced-mode short-circuited line. This results in a reduction in the (inaccessible) difference port reflection and a corresponding increase of the

Manuscript received August 29, 1966; revised November 9, 1966. This work was submitted as a report in partial fulfillment of the requirements for the M.S.E.E. degree at the Polytechnic Institute of Brooklyn, Brooklyn, N. Y.; the experimental work was supported by Wheeler Labs., Inc.

[1] K. I. Parad and R. L. Moynihan, "Split-tee power divider," *IEEE Trans. on Microwave Theory and Techniques*, vol. MTT-13, pp. 91-95, January 1965.

[2] R. A. Kaplan, "Three-port VHF coaxial-hybrid power divider, model 388," Wheeler Labs. Inc., Great Neck, N. Y., unpublished rept. 852 to Sylvania Electric Products, Inc., February 26, 1959.